The Analyst

Quantitative Analysis of Sulfated Calcium Carbonates Using Raman Spectroscopy and X-ray Powder Diffraction

Christos G. Kontoyannis*†, Malvina G. Orkoula and Petros G. Koutsoukos

ICE/HT-FORTH and Department of Pharmacy, University of Patras, University Campus, GR 26500 Patras, Greece

A non-destructive method based on the use of Raman spectroscopy (RS) for the determination of the percentage of gypsum in sulfated marble is presented. The Raman spectra of well mixed powder samples of calcite–aragonite, calcite–gypsum and gypsum–aragonite pairs of mixtures were recorded and the characteristic bands at 280 cm^{-1} for calcite, 205 cm^{-1} for aragonite and 412 cm^{-1} for gypsum were used as the basis for the quantitative analysis of specimens in which the most stable calcium carbonate phases, calcite and aragonite, were present. The detection limits were found to be 0.3 mol% for calcite, 0.5 mol% for aragonite and 0.6 mol% for gypsum. For samples containing only one calcium carbonate phase the use of the strong and sharp Raman band at 1085 cm^{-1}, common for aragonite and calcite, together with the intensity of the Raman peak at 1006 cm^{-1} for gypsum, yielded lower detection limits: calcite 0.1, aragonite 0.1 and gypsum 0.05 mol%. The analysis by RS was compared with X-ray powder diffraction (XRD). In this analysis, the calibration curves were constructed using the relative intensities corresponding to the 113, the 111 and the 12$\bar{1}$ reflections of the calcite, aragonite and gypsum, respectively. The detection limits for calcite, aragonite and gypsum were 4, 5 and 1–2 mol%, respectively. The potential of using RS for a point-by-point analysis ('mapping') of a surface by focusing the laser beam on the selected spots was also demonstrated on a marble sample removed from Athens National Garden, exposed in the open air.

Keywords: *Raman spectroscopy; calcium carbonate polymorphs; gypsum; X-ray powder diffraction*

Marble is a metamorphic rock formed from limestone by geological processes involving high temperatures and high pressures. Limestone, in turn, is a calcium carbonate rock built up from the sedimentation of marine organisms over millions of years. Marble sulfation has been the subject of many investigations in the recent past, ranging from studies of field samples[1,2] to laboratory investigations using synthetic atmospheric environments enriched in SO_2.[3–5] Atmospheric pollution has been accused of causing the deterioration of calcium carbonate stones and several mechanisms, leading to the conversion of $CaCO_3$ into $CaSO_4 \cdot 2H_2O$, have been proposed.[2,6–8]

The development of a technique for monitoring the progress of marble sulfation on important cultural monuments in a non-destructive manner is needed. Commonly used methods include the employment of classical elemental analysis (CEA),[6] scanning electron microscopy (SEM),[1,6,9] X-ray powder diffraction (XRD),[1,9] petrographic microscopy (PM)[6,9] and atomic absorption spectrometry (AAS).[6] Some of these methods are used for identification purposes only (SEM, PM), others are destructive for the sample (CEA, XRD, SEM, PM, AAS) and others are suitable for elemental analysis only and not for the determination of the species present (CEA, AAS).

The potential presence of the two commonly encountered crystal phases of calcium carbonate, calcite and aragonite, in the specimen[10,11] complicates the analytical problem. The identification of these two phases and the determination of the respective percentages can be accomplished through the use of vibrational spectroscopic techniques such as infrared (IR) and Raman spectroscopy (RS). Although the IR determination of the calcite to aragonite ratio has been reported,[12,13] disadvantages of this method include broadness of inorganic absorption bands and specimen preparation involving grinding or pelleting, which can lead to the conversion of aragonite into calcite. RS is a non-destructive technique which has already been used for the identification of calcium carbonate phases[14] with the potential for *in situ* application using fibre optics. This method however, to our knowledge, has not yet been applied to the quantitative analysis of sulfated calcareous rocks. In this work, the possibility of using RS as a non-destructive technique for the determination of the gypsum content in marble, was investigated and the results were compared with those obtained by application of quantitative XRD analysis.[15]

Experimental

Preparation of Chemicals and Samples

Pure aragonite crystals were prepared by the simultaneous dropwise addition of 5 ml of a solution of 1 mol l^{-1} $Ca(NO_3)_2$ (Ferak, Berlin, Germany) at 90 °C and 5 ml of 1 mol l^{-1} $(NH_4)_2CO_3$ (Ferak) at 45 °C into 200 ml of triply distilled water at 95 °C. The solution, during precipitation, was saturated with CO_2 by bubbling the gas through the slurry. The crystals, in the form of a slurry, were filtered (Millipore, Bedford, MA, USA; 0.22 μm) and washed with triply distilled water at 90 °C and with absolute ethanol at room temperature. The powder was dried at 80 °C for 1 h and stored in a desiccator.

Calcite powder was prepared as follows: 1 l of 1 mol l^{-1} $(NH_4)_2CO_3$ solution was added dropwise to 1 l of 1 mol l^{-1} $Ca(NO_3)_2$ solution and stirred magnetically at ambient temperature. The suspension was incubated in the mother liquor for 15 d. Next, it was filtered through membrane filters and washed with triply distilled water at 70 °C. The crystals were dried at 120 °C for 2 d and stored in a desiccator.

Gypsum powder was prepared by adding 1 l of 0.1 mol l^{-1} Na_2CO_3 solution (Merck, Darmstadt, Germany) to 1 l of 0.1 mol l^{-1} $Ca(NO_3)_2$ solution stirred magnetically at 70 °C. Next, the slurry was filtered, washed with triply distilled water, resuspended and aged at 70 °C for 15 d with stirring. It was then filtered again, washed, dried at 120 °C for 2 d and stored in a dessicator.

The calcite, aragonite and gypsum crystals were characterized by IR spectroscopy, XRD, and SEM (JEOL, Tokyo, Japan; JSM 5200).

† Present address: Institute of Chemical Engineering and High Temperature Chemical Processes, University Campus, P.O. Box 1414, GR 26500, Patras, Greece.

In order to construct the calibration curves, carefully weighed mixtures of calcite–aragonite, aragonite–gypsum and gypsum–calcite, ranging from 0 to 100 mol% purity, were prepared from the respective solids. The solid mixtures were thoroughly mixed mechanically. The homogeneity of the mixed powders was verified by obtaining several Raman spectra for each mixture, focusing the laser beam at randomly selected parts of the surface.

Instrumentation

Raman spectroscopy (system configuration)

Raman spectra were excited by focusing 488 nm radiation from a 4 W Spectra-Physics (San Jose, CA, USA) argon laser on the marble sample and on the synthetically prepared mixtures. The plasma lines were removed from the laser beam by using a small monochromator as a filter. A cylindrical lens, with focal length 127 mm, was used to focus the laser line on the sample. The scattered light was collected at an angle of 90° and analysed with a Spex Industries (Edison, NJ, USA) Model 1403, 0.85 m double monochromator equipped with an RCA photomultiplier cooled to −20 °C and EG&G Ortec (Oak Ridge, TN, USA) photon-counting and electronic amplifier. The power of the incident laser beam was about 200 mW on the sample surface. Typical spectral resolution and time constant were 0.3 cm^{-1} and 3 s, respectively. The system was interfaced with a computer.

X-ray diffractometry

X-ray powder diffraction analysis was performed with a Philips (Eindhoven, The Netherlands, Model 1830/40 instrument) on finely powdered samples using Cu Kα radiation (40 kV and 30 mA) and an Ni filter with a scanning speed of 0.005° 2θ s^{-1}. The time constant was set at 2 s.

Results and Discussion

Theory for Construction of Raman Calibration Curve

The Raman spectra of calcite, aragonite and gypsum are shown in Fig. 1. The characteristic Raman bands due to the lattice vibration mode at 280, 205 and 412 cm^{-1} for calcite, aragonite and gypsum, respectively, and the ν_1 internal mode (symmetric stretching) at 1085 cm^{-1} for both calcite and aragonite[16,17] and at 1006 cm^{-1} for gypsum[16] are easily distinguished. The spectra are in good agreement with earlier reports.[18]

It is obvious that the Raman bands in the spectral region between 170 and 450 cm^{-1} should be used for the quantitative analysis of a mixture of calcite, aragonite and gypsum since the strong peak at 1085 cm^{-1}, which is attributed to the symmetric C–O stretching, is common for all calcium carbonate phases. On the other hand, when the specimen contains only one $CaCO_3$ phase and gypsum, the 1085 and 1006 cm^{-1} bands can also be used for quantitative analysis. In this case a lower detection limit is expected, since the analysis is based on stronger and sharper peaks. In the present work both possibilities were addressed by constructing Raman calibration curves using the bands of the spectral regions of interest, *i.e.*, 170–450 and 970–1110 cm^{-1}.

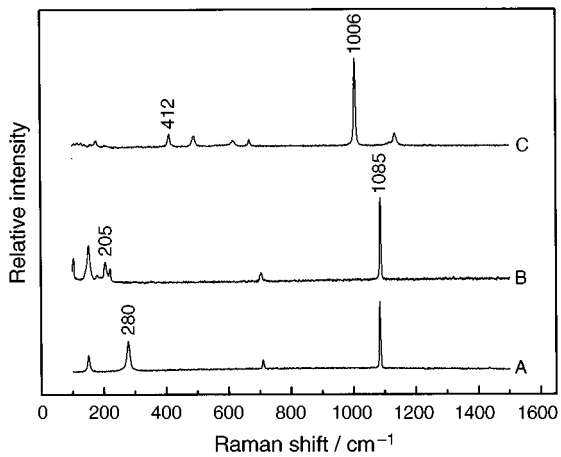

Fig. 1 Raman spectra of the synthetically prepared A, calcite, B, aragonite and C, gypsum.

The purpose was to find an easy and reliable method for calculating each ingredient's percentage and, therefore, peak heights were used and not integrated intensities of the bands.

The intensity of a Raman line depends on a number of factors, including incident laser power, frequency of scattered radiation, absorptivity of the materials involved in the scattering and the response of the detection system. Thus, the measured Raman intensity, $I(\nu)$, can be represented by[19]

$$I(\nu) = I_0 K(\nu) C \quad (1)$$

where I_0 is the intensity of the exciting laser radiation, ν is the Raman shift, $K(\nu)$ is a factor which includes the frequency-dependent terms (the over-all spectrophotometer response, the self-absorption of the medium and the molecular scattering properties) and C is the concentration of the Raman-active species.

Differences in the measured intensities of the various spectra obtained from the same specimen, which are attributed to factors such as the intensity variation of I_0 or the positioning of the sample, suggested the use of relative factors within each spectrum, *e.g.*, ratio of band intensities characteristic for each component. Thus, in a spectrum obtained from a sample in which several species are present, the ratio of the intensities of two peaks attributed to different compounds should be given by

$$\frac{I_A}{I_B} = \frac{K_A}{K_B} \times \frac{x_A}{x_B} \quad (2)$$

where the subscripts A and B indicate the different components and x_A/x_B is the molar fraction ratio of the two species. Eqn. (2) is valid only when there is no chemical interaction between the substances present in the sample. From eqn. 2, it is apparent that a plot of I_A/I_B *versus* x_A/x_B should yield a straight line with slope K_A/K_B. In the frequency range of the spectral measurements, the over-all spectrometer response may be considered to be constant, hence the K ratios are dependent only on the scattering parameter associated with each band, assuming that no significant absorption of the exciting radiation occurs. Consequently, the values assigned to the K ratio may be used regardless of the Raman spectroscopic system, provided that 488 nm radiation from an argon laser is used.

Raman Calibration Lines

For an aragonite–calcite mixture, eqn. (2) may be rewritten for the 280 cm^{-1} peak of calcite and the 205 cm^{-1} peak of aragonite as follows:

$$\frac{I_c^{280}}{I_a^{205}} = \frac{K_c^{280}}{K_a^{205}} \times \frac{x_c}{x_a} \quad (3)$$

where the subscripts c and a represent the calcite and the aragonite crystal phases, respectively, and the superscripts 280 and 205 are the wavenumbers of the respective Raman bands. The plot of I_c^{280}/I_a^{205} *versus* x_c/x_a is shown in Fig. 2. The

equation for the calibration line was obtained by linear regression of the experimental data:

$$\frac{I_c^{280}}{I_a^{205}} = 1.646 \times \frac{x_c}{x_a} \quad (4)$$

The correlation coefficient (r), was 0.999 997 and the standard deviation (s), for the slope and the intercept were 1.4×10^{-3} and 4.9×10^{-2}, respectively. Assuming that $x_a + x_c = 1$, the RSD for $x_a = 0.4$ was found to be 3.3%, and the detection limits (DL) for calcite and aragonite were calculated to be of the order of 0.3 and 0.5%, respectively.

Similarly, calibration lines for calcite–gypsum and aragonite–gypsum mixtures were constructed using the Raman bands at 280 and 1085 cm^{-1} for calcite, 412 and 1006 cm^{-1} for gypsum and 205 and 1085 cm^{-1} for aragonite. Typical spectra of the various mixtures are shown in Fig. 3. The cumulative information for the RS calibration lines appear in Table 1.

Calculation of the Molar Fraction of Calcite, Aragonite and Gypsum in a Sample Using the Raman Calibration Curves

Two-component systems

The gypsum–calcite and the gypsum–aragonite mixtures belong to this category. The stronger Raman bands at 1085 cm^{-1} for either the calcite or aragonite phases and at 1006 cm^{-1} for gypsum can be used [eqn. (7) and (8) in Table 1].

For the calcite–gypsum mixtures and assuming that $x_g + x_c = 1$, eqn. (7) can be transformed to

$$x_g = \frac{0.721 I_g^{1006}}{I_c^{1085} + 0.721 I_g^{1006}} \quad (9)$$

Similarly, for the aragonite–gypsum system, eqn. (8) can be rewritten as

$$x_g = \frac{0.748 I_g^{1006}}{I_a^{1085} + 0.748 I_g^{1006}} \quad (10)$$

Three-component systems

This case applies to sulfated calcareous rocks in which both calcium carbonate phases are present together with gypsum. The calibration lines used in the two-component system case cannot be used since both aragonite and calcite exhibit a strong peak at the same frequency, 1085 cm^{-1}. Eqns. (4), (5) and (6) in Table 1 were used instead. Assuming that $x_a + x_g + x_c = 1$,

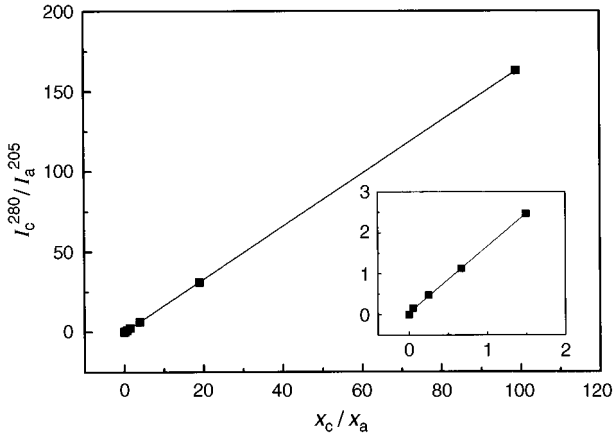

Fig. 2 Raman calibration line for calcite–aragonite mixtures.

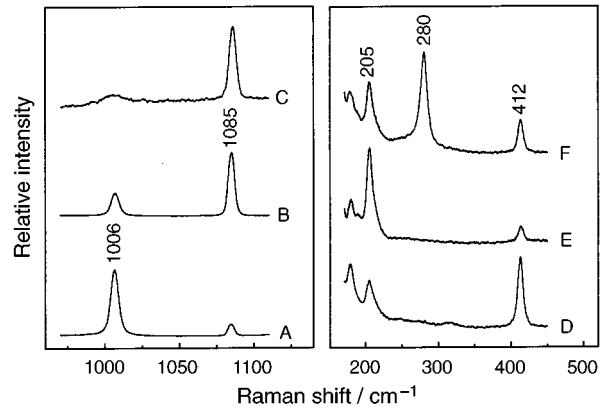

Fig. 3 Raman spectra of: A, 20 mol% calcite–80 mol% gypsum; B, 80 mol% calcite–20 mol% gypsum; C, sulfated marble sample; D, 20 mol% aragonite–80 mol% gypsum; E, 80 mol% aragonite–20 mol% gypsum; and F, 40 mol% calcite–30 mol% aragonite–30 mol% gypsum.

Table 1 Cumulative results for the RS calibration curves

Eqn. No.	Calibration line	r	s of slope	s of intercept	RSD (%)	DL (mol%)
(4)	$\frac{I_c^{280}}{I_a^{205}} = 1.646 \times \frac{x_c}{x_a}$	0.999 997	1.4×10^{-3}	4.9×10^{-2}	3.3 ($x_a = 0.4$)	Calcite 0.3 Aragonite 0.5
(5)	$\frac{I_c^{280}}{I_g^{412}} = 1.912 \times \frac{x_c}{x_g}$	0.999 94	8.7×10^{-3}	6×10^{-2}	3.3 ($x_g = 0.4$)	Calcite 0.3 Gypsum 0.6
(6)	$\frac{I_a^{205}}{I_g^{412}} = 1.171 \times \frac{x_a}{x_g}$	0.999 08	2.3×10^{-2}	3.7×10^{-2}	3.0 ($x_g = 0.4$)	Aragonite 0.5 Gypsum 0.6
(7)	$\frac{I_c^{1085}}{I_g^{1006}} = 0.721 \times \frac{x_c}{x_g}$	0.999 97	2.2×10^{-3}	1.4×10^{-2}	2.0 ($x_g = 0.4$)	Calcite 0.1 Gypsum 0.05
(8)	$\frac{I_a^{1085}}{I_g^{1006}} = 0.748 \times \frac{x_a}{x_g}$	0.999 99	1.7×10^{-3}	1.1×10^{-2}	1.7 ($x_g = 0.4$)	Aragonite 0.1 Gypsum 0.05

the molar fractions in a sample may be determined from the following relationships:

$$x_a = \frac{1.646 I_a^{205}}{I_c^{280} + 1.646 I_a^{205} + 1.927 I_g^{412}} \quad (11)$$

$$x_c = \frac{I_c^{280}}{1.646 I_a^{205}} \times x_a \quad (12)$$

$$x_g = \frac{1.171 I_g^{412}}{I_a^{205}} \times x_a \quad (13)$$

The validity of these expressions was tested on the spectrum recorded from a powder mixture consisting of 40 mol% calcite, 30 mol% aragonite and 30 mol% gypsum [Fig. 3(F)]. The results were calcite 39.7, aragonite 30.9 and gypsum 29.4 mol%. The deviation of the results obtained was within the experimental error (*s* in Table 1).

It should be noted that the analytical methodology presented here does not depend on the simultaneous existence of the calcium carbonate phases and the gypsum, since there is neither chemical interaction between these species nor overlap of the corresponding bands in the Raman spectra. As a result, the relative intensities used in the analysis are not affected. Moreover, as may be seen from eqn. (1), the intensity of the Raman bands depends on the concentration of the investigated species alone.

If an additional compound, besides gypsum, aragonite and/or calcite, is also present and provided that this does not contribute to the RS signal at the proposed frequencies and that there is no chemical interaction among the species present, eqns. (4)–(8) are still valid and the ratio of the gypsum to the calcium carbonate phases can be determined.

Theory for Construction of XRD Calibration Curve

The XRD spectra of calcite, aragonite and gypsum are shown in Fig. 4. The calcite spectrum exhibits two major peaks associated with the 104 and 113 reflections. Unfortunately, the former coincides with a gypsum peak, so only the intensity of the 113 reflection was used. The peaks attributed to the $12\bar{1}$ and 111 reflections of gypsum and aragonite, respectively, were also used for the quantitative analysis.

If the sample is a uniform mixture of two components and extinction and microabsorption effects are neglected, it can be shown that[20]

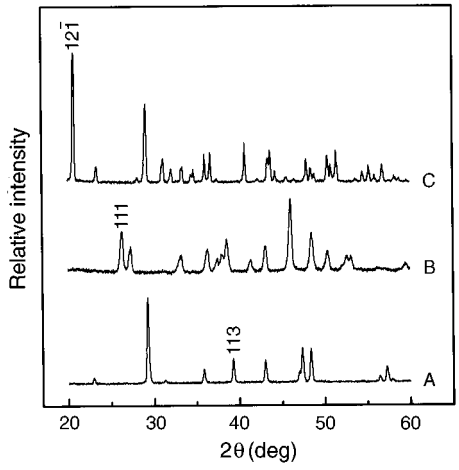

Fig. 4 XRD spectra of the synthetically prepared A, calcite, B, aragonite and C, gypsum.

$$\frac{I_A}{I_B} = \Lambda \times \frac{x_A}{x_B} \quad (14)$$

where Λ is a proportionality constant which depends on the component, the diffraction line and the mass absorption coefficient of the species present. I_A/I_B represents the ratio of the intensities of two selected diffraction lines in a mixture of two substances, and x_A/x_B is the molar fraction ratio of the two substances. A plot of I_A/I_B *versus* x_A/x_B should yield a straight line with an intercept of zero.

XRD Calibration Lines

Calibration curves for calcite–aragonite, aragonite–gypsum and gypsum–calcite binary mixtures were constructed.

For gypsum–aragonite mixtures the plot of $I_a^{111}/I_g^{12\bar{1}}$ *versus* x_a/x_g, where the subscripts a and g represent gypsum and aragonite, respectively, and the superscripts the XRD reflections, as shown in Fig. 5. The equation for the calibration line was obtained by linear regression of the experimental data:

$$\frac{I_a^{111}}{I_g^{12\bar{1}}} = 0.18 \times \frac{x_a}{x_g} \quad (15)$$

The correlation coefficient (*r*) was 0.9993 and the *s* for the slope and the intercept were 3×10^{-2} and 2.3×10^{-2}, respectively. Assuming that $x_a + x_g = 1$, the RSD for $x_g = 0.4$ was found to be 12.2%, and DL for gypsum and aragonite were calculated to be of the order of 1–2 and 5%, respectively.

Similarly, calibration lines were constructed for calcite–gypsum and aragonite–calcite mixtures using the XRD reflection peaks of 113, $12\bar{1}$ and 111 for calcite, gypsum and aragonite, respectively. Representative spectra are shown in Fig. 6. The cumulative information for the XRD calibration lines is given in Table 2.

Calculation of the Molar Fraction of Calcite, Aragonite and Gypsum in a Ternary Sample using the XRD Calibration Curves

Assuming that $x_a + x_g + x_c = 1$ and by employing eqns. (15), (16) and (17) in Table 2, the molar fractions in a sample in which calcite, aragonite and gypsum are present can be determined using the following relationships:

$$x_a = \frac{1.13 I_a^{111}}{1.13 I_a^{111} + I_c^{113} + 0.20 I_g^{12\bar{1}}} \quad (18)$$

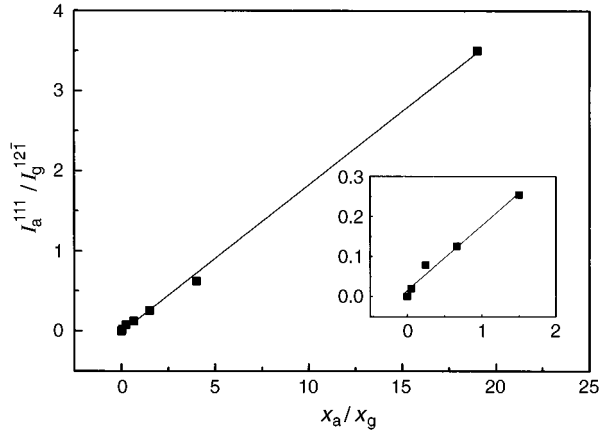

Fig. 5 XRD calibration line for gypsum–aragonite mixtures.

Table 2 Cumulative results for the XRD calibration lines

Eqn. No.	Calibration line	r	s of slope	s of intercept	RSD (%)	DL (mol%)
(15)	$\frac{I_a^{111}}{I_g^{12\bar{1}}} = 0.18 \times \frac{x_a}{x_g}$	0.9993	3×10^{-2}	2.3×10^{-2}	12.2 (x_g = 0.4)	Aragonite 5 Gypsum 1–2
(16)	$\frac{I_c^{113}}{I_g^{12\bar{1}}} = 0.18 \times \frac{x_c}{x_g}$	0.9853	1.5×10^{-2}	2.7×10^{-2}	13.3 (x_g = 0.4)	Calcite 4 Gypsum 1–2
(17)	$\frac{I_c^{113}}{I_a^{111}} = 1.13 \times \frac{x_c}{x_a}$	0.9991	2.4×10^{-2}	4.2×10^{-2}	11.2 (x_a = 0.4)	Calcite 4 Aragonite 5

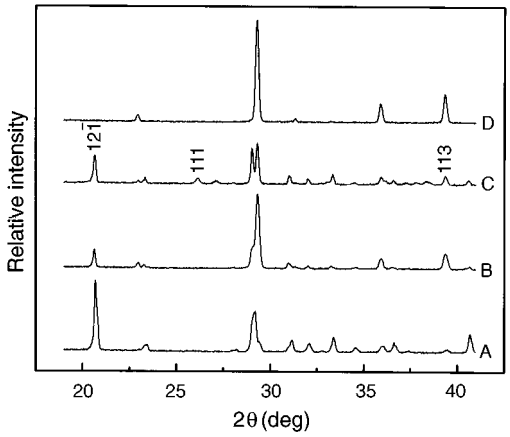

Fig. 6 XRD spectra of: A, 20 mol% calcite–80 mol% gypsum; B, 80 mol% calcite–20 mol% gypsum; C, 40 mol% calcite–30 mol% aragonite–30 mol% gypsum; and D, sulfated marble sample.

$$x_c = \frac{I_c^{113}}{1.13 I_a^{111}} \times x_a \quad (19)$$

$$x_g = \frac{0.18 I_g^{12\bar{1}}}{I_a^{111}} \times x_a \quad (20)$$

The validity of the expressions derived for the XRD technique was also tested on a spectrum recorded from the same ternary powder mixture as used for testing the Raman calibration curves, Fig. 6(C). The percentages determined were calcite 41.9, aragonite 30.8 and gypsum 27.3 mol%. The deviation of the results obtained was within the experimental error (s in Table 2).

As mentioned for the RS method, the presence of a fourth compound does not affect the validity of the derived equations provided that there is no chemical interaction among the species present or overlap of the XRD peaks used for the analysis with the XRD lines of the additional species.

Application to a Sulfated Marble Sample

A marble sample taken from Athens National Garden was tested for gypsum using the techniques described here.

Raman spectra were excited from several points of the marble surface. Only calcite and gypsum were present [Fig. 3(C)]. Application of eqn. (9) yielded gypsum concentrations between 0 and 8.5 mol%.

An external layer from sample surface was removed mechanically and the XRD spectrum was recorded [Fig. 6(D)]. No detectable gypsum was found. This result was expected because only the average percentage from the removed surface layer can be observed with the XRD technique, and the possibility of having material from the inner marble layer, consisting of pure calcite only, in the powder collected from the surface is not trivial. Hence the percentage of gypsum in the XRD-tested material was below the detection limit.

Comparison Between RS and XRD

Both techniques were used for the determination of the percentage of gypsum on a calcium carbonate surface, and RS exhibited certain advantages over the XRD method: (a) RS was non-destructive for the sample and less time consuming; (b) reliable point-by-point analysis ('mapping') of the surface was accomplished using RS, whereas XRD yielded only the average percentage of the bulk, ground powder sample; and (c) from the comparison of the calibration line statistics (Tables 1 and 2) it can be seen that RS exhibited lower SD and lower DL than the XRD calibration curves.

Conclusions

Methods based on RS and XRD for quantitative determination of the transformation of the surface of monuments into gypsum, known as marble deterioration, were developed. Calibration curves from mixtures of calcite and aragonite (the most stable phases of calcium carbonate), and gypsum were constructed. The much lower detection limits given by RS, the fact that it is non-destructive and the potential use of the technique for chemical mapping of the marble surface are among the major advantages of the RS over powder XRD.

The authors are indebted to Professor G.N. Papatheodorou for helpful suggestions and for providing the experimental facilities. They thank Dr. P. Klepetsanis for kindly supplying the gypsum powder. Partial support of this work by the GSRT EPET II Program (contract No. 368/11-1-95) is gratefully acknowledged.

References

1 Camuffo, D., Del Monte, M., Sabbioni, C., and Vittori, O., *Atmos. Environ.*, 1982, **16**, 2253.
2 Ross, M., McGee, E. S., and Ross, D. R., *Am. Mineral.*, 1989, **74**, 367.
3 Skoulikidis, T., and Charalambous, D., *Br. Corros. J.*, 1981, **16**, 70.
4 Johanson, L. G., Lindqvist, O., and Mangio, R., *Durability Build. Mater.*, 1988, **5**, 439.
5 Gauri, K. L., Chowdhury, A. N., Kulshreshta, N. P., and Punuru, A. R., *Stud. Conserv.*, 1989, **34**, 201.
6 Verges-Belmin, V., *Atmos. Environ.*, 1994, **28**, 295.
7 Van Houte, G., Rodrique, L., Genet, M., and Delmon, B., *Environ. Sci. Technol.*, 1981, **15**, 327.
8 Lipfert, F. W., *Atmos. Environ.*, 1989, **23**, 415.
9 Gauri, K. Lal, and Holdren G. C., Jr., *Environ. Sci. Technol.*, 1981, **15**, 386.
10 Berner, R. A., *Am. J. Sci.*, 1966, **264**, 1.

11 Hacker, B. R., Kirby, S. H., and Bohlen, S. R., *Science*, 1992, **258**, 110.
12 Compere, E. L., and Bates, J. M., *Limnol. Oceanogr.*, 1973, **18**, 326.
13 Xyla, A., and Koutsoukos, P. G., *J. Chem. Soc., Faraday Trans. 1*, 1989, **85**, 3165.
14 Herman, R. G., Bogdan, C. E., Sommer, A. J., and Simpson, D. R., *Appl. Spectrosc.*, 1987, **41**, 437.
15 Silk, S. T., and Lewin, S. Z., *Adv. X-ray Anal.*, 1971, **14**, 29.
16 Griffith, P. G., in *Spectroscopy of Inorganic-based Materials*, eds. Clark, R. J. H., and Hester, R. E., Wiley, Chichester, 1987, pp. 137 and 151.
17 Behrens, G., Kuhn, L. T., Ubic R., and Heuer, A. H., *Spectrosc. Lett.*, 1995, **28**, 983.
18 Degen, A., and Newman, G. A., *Spectrochim. Acta, Part A*, 1993, **49**, 859.
19 Strommen, D., and Nakamoto, K., in *Laboratory Raman Spectroscopy*, Wiley, New York, 1984, pp. 71–75.
20 Whiston, C., in *X-ray Methods*, Wiley, New York, 1987, p. 113.

Paper 6/06167B
Received September 9, 1996
Accepted September 24, 1996